Pharmaceutical Research, Vol. 26, No. 8, August 2009 (© 2009)
DOI: 10.1007/s11095-009-9905-3

Research Paper

Novel Inhibitors of Human Organic Cation/Carnitine Transporter (hOCTN2) *via* Computational Modeling and *In Vitro* Testing

Lei Diao,[1] Sean Ekins,[1,2,3] and James E. Polli[1,4]

Received February 19, 2009; accepted May 4, 2009; published online May 13, 2009

Purpose. The objective was to elucidate the inhibition requirements of the human organic cation/carnitine transporter (hOCTN2).
Methods. Twenty-seven drugs were screened initially for their potential to inhibit uptake of L-carnitine into a stably transfected hOCTN2-MDCK cell monolayer. A HipHop common features pharmacophore was developed and used to search a drug database. Fifty-three drugs, including some not predicted to be inhibitors, were selected and screened *in vitro*.
Results. A common features pharmacophore was derived from initial screening data and consisted of three hydrophobic features and a positive ionizable feature. Among the 33 tested drugs that were predicted to map to the pharmacophore, 27 inhibited hOCTN2 *in vitro* (40% or less L-carnitine uptake from 2.5 μM L-carnitine solution in presence of 500 μM drug, compared to L-carnitine uptake without drug present). Hence, the pharmacophore accurately prioritized compounds for testing. K_i measurements showed low micromolar inhibitors belonged to diverse therapeutic classes of drugs, including many not previously known to inhibit hOCTN2. Compounds were more likely to cause rhabdomyolysis if the C_{max}/K_i ratio was higher than 0.0025.
Conclusion. A combined pharmacophore and *in vitro* approach found new, structurally diverse inhibitors for hOCTN2 that may possibly cause clinical significant toxicity such as rhabdomyolysis.

KEY WORDS: carnitine; human organic cation/carnitine transporter (hOCTN2); pharmacophore; rhabdomyolysis.

INTRODUCTION

The human organic cation/carnitine transporter (hOCTN2) is a high affinity cation/carnitine transporter widely expressed in human tissues, including skeletal muscle and kidney (1). hOCTN2 is physiologically important for maintaining the homeostasis of the endogenous compound L-carnitine which is involved in intermediary metabolism (2). The primary role of hOCTN2 is to facilitate the transport of long-chain fatty acids into mitochondria for β-oxidation and subsequent energy production. The mutation of the hOCTN2 gene in humans is also known to cause primary systemic carnitine deficiency with clinical symptoms that include hypoketotic hypoglycemia, cardiomyopathy, and skeletal myopathy (3,4).

HMG-CoA reductase inhibitors, alone or in combination with other medications, are well known to be associated with rhabdomyolysis, a relatively rare condition resulting in a form of muscle weakness (5). Cerivastatin was withdrawn from the US market due to this side effect. The Food and Drug Administration (FDA) also recently issued an alert on the risk of rhabdomyolysis when simvastatin is used with amiodarone. However, the mechanism of muscle injury by HMG-CoA reductase inhibitors is still poorly defined. One possible mechanism involves the inhibition of L-carnitine uptake into muscle and/or inhibition of L-carnitine re-absorption in the kidney, both mediated by hOCTN2. An understanding of the inhibition requirements of hOCTN2 has potential to predict hOCTN2 inhibitors and potential utility in predicting drug-induced secondary carnitine deficiency.

Several reports have identified cationic or zwitterionic drugs as inhibitors and/or substrates of OCTN2 (6–8,11). However, a systemic approach to study the molecular requirements of OCTN2 inhibition is lacking. In the current study, a pharmacophore was developed to identify the molecular features required for hOCTN2 inhibition. Twenty-seven drugs were initially screened for *in vitro* hOCTN2 inhibition. A common features pharmacophore was subsequently developed and then applied to search a database of

Electronic supplementary material The online version of this article (doi:10.1007/s11095-009-9905-3) contains supplementary material, which is available to authorized users.

[1] Department of Pharmaceutical Sciences, School of Pharmacy, University of Maryland, Baltimore, Maryland 21201, USA.
[2] Collaborations in Chemistry, Jenkintown, Pennsylvania 19046, USA.
[3] Department of Pharmacology, Robert Wood Johnson Medical School, University of Medicine and Dentistry of New Jersey, Piscataway, New Jersey 08854, USA.
[4] To whom correspondence should be addressed. (e-mail: jpolli@rx.umaryland.edu)

ABBREVIATIONS: MDCK, Madin–Darby canine kidney; OCTN2, organic cation/carnitine transporter; QSAR, quantitative structure activity relationship.

796 compounds. The pharmacophore, which consisted of three hydrophobic and a positive ionizable feature, identified potential hOCTN2 inhibitors from the database. Experimental testing was conducted on 53 additional compounds to further test the pharmacophore. Among 33 drugs that were predicted to be inhibitors and tested, 27 were observed to be active. Diverse therapeutic classes of drugs were found to be novel potent inhibitors of hOCTN2.

MATERIALS AND METHODS

Materials

L-[^{3}H]carnitine was purchased from American Radiolabeled Chemicals (St. Louis, MO). Fetal bovine serum, trypsin, and Dulbecco's modified Eagle medium (DMEM) were purchased from Invitrogen Corporation (Carlsbad, CA). L-carnitine, all drugs, and other chemicals were obtained from Sigma Chemical (St. Louis, MO), Alexis Biochemicals (San Diego, CA), AK Scientific (Mountain View, CA), LKT Labs (St. Paul, MN), Spectrum Chemicals & Laboratory Products (Gardena, CA), Spectrum Pharmacy Products (Tucson, AZ), or TCI America (Portland, OR). Stably transfected hOCTN2-MDCK cells were kindly provided by Xin Ming and Dr. Dhiren R. Thakker from the University of North Carolina-Chapel Hill.

Cell Culture

Stably transfected hOCTN2-MDCK cells were cultured at 37°C, 90% relative humidity, and 5% CO_2 atmosphere and fed every 2 days. Media was composed of DMEM supplemented with 10% FBS, 50 U/mL penicillin, and 50 μg/mL streptomycin. Cells were passaged after reaching 80% confluence.

hOCTN2-MDCK cells were seeded at a density of 0.7 million cells per square centimeter in 12-well plates (Corning; Corning, NY). To enhance hOCTN2 expression, cells were treated with 10 mM sodium butyrate for 12–15 h at 37°C prior to uptake or inhibition study.

Characterization of Stably Transfected hOCTN2-MDCK Cell Monolayer

Stably transfected hOCTN2-MDCK cells were characterized in terms of L-carnitine uptake. Uptake studies were performed at L-carnitine concentrations ranging from 0 to 200 μM and donor solutions were spiked with L-[^{3}H] carnitine. Buffer consisted of either Hank's balanced salts solution (HBSS) which contains 137 mM sodium chloride or a sodium-free, modified HBSS where sodium chloride was replaced with 137 mM tetraethylammonium chloride. Identical studies were conducted using sodium-containing buffer and sodium-free buffer, since hOCTN2-mediated uptake of L-carnitine is sodium-dependent. L-carnitine uptake was also performed in the presence of sodium using MDCK cells that were not transfected with hOCTN2.

At the end of the assay (10 min), active uptake was terminated by washing cells thrice with chilled sodium-free buffer. Cells were then lysed with 0.25 mL of 1 N NaOH for 4 h. Cell lysate was neutralized with 0.25 mL of 1 N HCl and counted for associated radioactivity using an LS6500 liquid scintillation counter (Beckman Instruments, Inc., Fullerton, CA).

A passive transport model (Eq. 1) was fitted to uptake data from sodium-free studies:

$$J = P_p S \tag{1}$$

where J is L-carnitine flux, P_p is the passive L-carnitine permeability coefficient, and S is L-carnitine concentration. The Michaelis–Menten model with parallel passive permeability (Eq. 2) was fitted to uptake data from sodium-containing studies:

$$J = \frac{J_{max} S}{K_t + S} + P_p S \tag{2}$$

where J_{max} and K_t are the Michaelis–Menten constants for hOCTN2-mediated transport.

Equations 1 and 2 were applied sequentially to sodium-free and sodium-containing uptake data to estimate P_p, K_t, and J_{max}. The P_p estimate from sodium-free studies was applied to Eq. 2.

hOCTN2 Inhibition Screening Studies

Twenty-seven drugs were initially screened for hOCTN2 inhibition. These compounds were selected since they are drugs and reflect diverse structures that are either weakly basic or neutral, and are commercially available. Cis-inhibition studies of L-carnitine (2.5 μM with spiked L-[^{3}H] carnitine) uptake were carried out using drug at a single concentration (500 μM) in sodium-containing buffer. At the end of the assay (10 min), active uptake was terminated by washing cells thrice with chilled sodium-free buffer. Cells were then lysed and quantified for radioactivity as described above. Results are expressed in terms of percent uptake of L-carnitine, compared to L-carnitine uptake without drug present.

Pharmacophore Development and Database Screening

The computational molecular modeling studies were carried out using Catalyst™ in Discovery Studio 2.0 or 2.1 (Accelrys, San Diego, CA) running on a Centrino Duo processor (Intel, Santa Clara, CA). Common features (HipHop) pharmacophore models attempt to describe the arrangement of key features that are important for biological activity and their generation has been widely described (9,10,12). Up to 255 molecule conformations were created for the following structures with the BEST conformer generation method, with the maximum energy threshold of 20 kcal/mol.

Pharmacophore common features were initially developed using verapamil and propantheline, which provided the highest inhibition from the inhibition screening studies. These common features served as the template molecules to which chlorpheniramine, diltiazem and imipramine were mapped (Supplemental Table I of the Electronic Supplementary Material). Hence, the pharmacophore was based on the five most active compounds that were screened. Physostigmine and guanfacine were also used as less active compounds whose features were excluded from the pharmacophore, in

order to highlight features of the five most active compounds. Physostigmine and guanfacine; chlorpheniramine, diltiazem and imipramine; and verapamil and propantheline were labeled principal 0, 1, and 2, respectively (Supplemental Table I of the Electronic Supplementary Material).

The SCUT database of 796 compounds (656 drugs in the SCUT 2008 database plus additional drug metabolites and drugs of abuse) was created using structures in the MDL SDF format prior to conversion to a 3D Catalyst database after generating up to 100 molecule conformations with the FAST conformer generation method, with the maximum energy threshold of 20 kcal/mol.

The common features pharmacophore was then applied to screen the SCUT database using the FAST search method, as previously described (13,14). The quality of the molecule mapping to the pharmacophore was determined by the FitValue which is dependent on the proximity of a compound to the pharmacophore feature centroids and the weights assigned to each centroid, where a higher FitValue represents a better fit.

An additional pharmacophore with shape restriction was developed and applied. This shape restriction involved the van der Waals shape of propantheline, which was the most active compound from the initial screen.

Experimental Testing of the Pharmacophore and Measurement of K_i Values

Pharmacophore database screening resulted in drugs that were predicted to strongly inhibit hOCTN2, as well as those predicted not to inhibit hOCTN2. Fifty-three drugs were subsequently selected and analyzed in this study. These drugs possessed a range of pharmacophore-predicted FitValues and were subjected to the hOCTN2 inhibition assay in order to test the pharmacophore. Inhibition studies were carried out as described above in the "hOCTN2 Inhibition Screening Studies" section. A few compounds which were not soluble at 500 μM were tested at a lower concentration as noted.

Inhibitory K_i values were measured for 14 drugs. Verapamil and propantheline K_i values were measured since these compounds were the most potent from the inhibition screening studies and contributed to pharmacophore development. The other 12 drugs were selected primarily based on the pharmacophore results since they collectively exhibited a range of percent inhibition and FitValues. To measure K_i, inhibition studies were performed as described above, where a range of drug concentrations were applied to inhibit L-carnitine (2.5 μM spiked with L-[^{3}H] carnitine) uptake. The following competitive inhibition model was applied:

$$J = \frac{J_{max}S}{K_t\left(1 + {}^{I}/_{K_i}\right) + S} + P_pS \quad (3)$$

where K_i is the competitive inhibition coefficient, I is the concentration of inhibitor, and S is the concentration of L-carnitine (i.e. 2.5 μM). In applying Eq. 3, only K_i was estimated. The other three parameters (i.e. J_{max}, K_t, and P_p) were estimated from L-carnitine uptake studies without inhibitor using Eqs. 1 and 2.

Vinblastine, the most potent inhibitor, was subjected to Lineweaver–Burk analysis where both vinblastine (0, 50, and 100 μM) and L-carnitine (1, 2.5, and 5 μM) concentrations were varied (15). Inhibition studies of L-carnitine by vinblastine were performed as described above. The competitive inhibition model (i.e. Eq. 3) was fit to the data. The non-competitive inhibition model (i.e. Eq. 4) was also fit to the data:

$$J = \frac{J_{max}S \Big/ \left(1 + \frac{I}{K_{i,n}}\right)}{K_t + S} + P_pS \quad (4)$$

where $K_{i,n}$ is the non-competitive inhibition coefficient. The Akaike Information Criterion (AIC) was used in selecting Eq. 3 or Eq. 4 as the better fitting model.

Data Analysis

Percent uptake in presence of drug was expressed as mean±SEM derived from three independent wells for each concentration of inhibitor, compared to L-carnitine uptake in absence of drug. Nonlinear curve fitting was performed using WinNonlin 4.1 (Pharsight, Mountain View, CA). Statistical analysis between C_{max}/K_i ratio and rhabdomyolysis was performed using Pearson's chi-square (χ^2) test in MINITAB version 14.11.1 (Minitab Inc., State College, PA). The criterion of significance was $p<0.05$.

RESULTS

Characterization of *l*-Carnitine Uptake into Stably Transfected hOCTN2-MDCK Cells

To confirm the expression of functional carnitine transport activity in hOCTN2-MDCK cells, L-carnitine uptake was measured in the presence and absence of sodium. In Fig. 1, the uptake of L-carnitine in the presence of sodium demonstrated saturable kinetics in the substrate range of 0–200 μM, while the uptake of L-carnitine in the absence of sodium demonstrated linear kinetics. In the absence of sodium, lower L-carnitine uptake was observed, in comparison to studies with sodium. Fitted K_m and V_{max} were 5.33±0.54 μM and 0.808±0.019 pmol/s/cm^2, respectively. The passive permeability of L-carnitine across hOCTN2-MDCK cells in the absence of

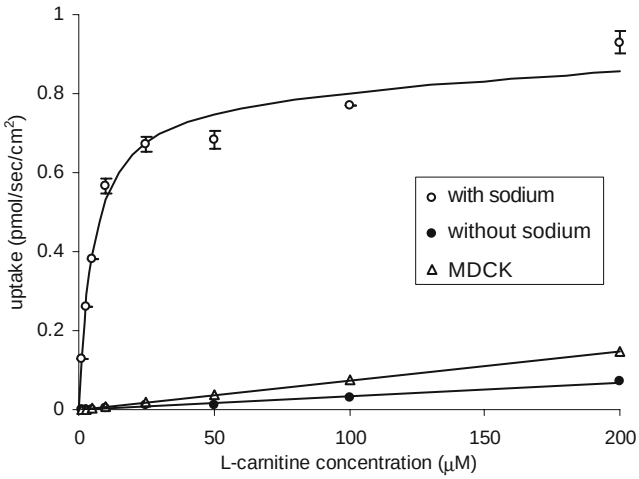

Fig. 1. Uptake of L-carnitine into hOCTN2-MDCK cells. Uptake was L-carnitine concentration-dependent in the presence of sodium. In the absence of sodium and in untransfected MDCK cells, L-carnitine uptake was low and not concentration-dependent.

sodium was a low $0.344\pm0.003\times10^{-6}$ cm/s. The uptake of L-carnitine into untransfected MDCK cells was also low and exhibited a passive permeability of $0.736\pm0.011\times10^{-6}$ cm/s.

Initial Screening of 27 Drugs as Inhibitors of hOCTN2

Twenty-seven drugs were initially screened for inhibition of L-carnitine uptake into hOCTN2-MDCK cells. A wide range of inhibition potency was found, from 7.43±0.19% uptake to 100±3% uptake, compared to L-carnitine uptake without drug present (Table I). The five most potent inhibitors from this initial screening were propantheline, verapamil, chlorpheniramine, diltiazem and imipramine (i.e. italicized compounds in Table I).

HipHop Common Features Pharmacophore Development

A common features pharmacophore was developed using propantheline and verapamil as the template molecules, to which chlorpheniramine, imipramine, diltiazem were mapped. Physostigmine and guanfacine were applied as less active compounds whose features were excluded from the pharmacophore, in order to highlight features of the five most active compounds. Supplemental Table I of the Electronic Supplementary Material lists molecules used in the HipHop pharmacophore and pharmacophore settings. The resulting HipHop pharmacophore consisted of three hydrophobic features and a positive ionizable feature (Fig. 2A). The hydrophobic features radiate from a positive ionizable feature with distances of ~7 to 9.4 Å (Supplemental Figure I of the Electronic Supplementary Material); the five most potent screened inhibitors each mapped to the pharmacophore (Fig. 2A, B). Physostigmine and guanfacine did not map to the pharmacophore. This approach was used in order to train the model to focus on the five most active compounds and exclude the features in physostigmine and guanfacine from this model.

Table I. List of 27 Compounds Initially Screened as hOCTN2 Inhibitors

Compound name	Percent L-carnitine uptake compared to control[a]
Propantheline	7.43±0.19
Verapamil	9.49±0.18
Chlorpheniramine	14.2±0.4
Diltiazem	15.5±0.4
Imipramine	16.9±1.4
Physostigmine	38.3±3.1
Propanolol	45.7±0.5
Guanfacine	46.2±3.3
Lidocaine	48.8±3.3
Ranitidine	54.0±1.2
Nicardipine	57.4±1.3
Labetalol	67.5±2.6
Bupropion	72.5±1.2
Bretylium tosylate	73.6±1.3
Mementine	74.4±2.9
Rifampin	77.6±4.3
Selegiline	78.7±2.2
Zidovudine	86.5±1.8
Lamivudine	88.6±3.9
Eyrthromycin	89.6±2.4
Atropine	92.3±3.5
Hydrochlorothiazide	92.5±0.6
Guanosine	93.3±1.4
Acyclovir	93.9±2.7
Sulfanilamide	95.2±5.5
Atenolol	96.0±5.5
Pramipexole	100±3

Cis-inhibition studies of L-carnitine (2.5 μM with spiked L-[^{3}H] carnitine) uptake were carried out using drug at a single concentration (500 μM) in sodium-containing buffer. Results are expressed in terms of percent uptake of L-carnitine, compared to L-carnitine uptake without drug present. The five most potent (italicized font) were used to derive the pharmacophore

[a] Control is uninhibited uptake of L-carnitine, which was 0.190± 0.006 pmol/s/cm^2. The concentrations of L-carnitine and screened drug were 2.5 and 500 μM, respectively

SCUT Database Screening Using the Developed Pharmacophore

The common features pharmacophore without shape restriction was used to search the database of 796 compounds and identified 136 molecules as potential inhibitors (Supplemental Table II of the Electronic Supplementary Material). Four of the five inhibitors that were used to build the model were retrieved from the database as potential inhibitors (i.e. verapamil, chlorpheniramine, imipramine and diltiazem, but interestingly not propantheline). For each compound in the database that was identified as a potential inhibitor, a FitValue was computed. A higher FitValue anticipates greater inhibition. A second pharmacophore, denoted the pharmacophore with shape restriction, was made more restrictive by adding the van der Waals volume around propantheline (Fig. 2C). This pharmacophore with shape restriction resulted in only 49 compounds as potential inhibitors and returned only imipramine from the five pharmacophore compounds (Supplemental Table III of the Electronic Supplementary Material).

In Vitro Testing of Selected Drugs from SCUT Database Screening

Fifty-three drugs were selected to test the pharmacophore via *in vitro* inhibition of L-carnitine uptake. These compounds were selected due to commercial availability and their wide range of predicted inhibition (i.e. range from anticipated potent hOCTN2 inhibitors to those that did not map to the pharmacophore). Table II lists the 32 compounds that were tested from the list of 136 compounds retrieved by the pharmacophore without shape restriction as potential inhibitors. These 32 compounds were selected as likely inhibitors, but with a wide range of FitValues, and were commercially available. Table III lists an additional 21 compounds that were tested. These compounds were not retrieved by the pharmacophore search of the database. Rather, these compounds were carnitine mimics, compounds previously reported to inhibit OCTN2, or drugs that cause rhabdomyolysis. Hence, including the 27 compounds from the initial hOCTN2 inhibition screening, a total of 80 compounds were tested for hOCTN2 inhibition in this study. Trifluoperazine, with a high pharmacophore FitValue of 3.408, was the most potent inhibitor found from all single concentration inhibition studies, with a percent uptake of 0.24±0.03% [i.e. over 99% inhibition].

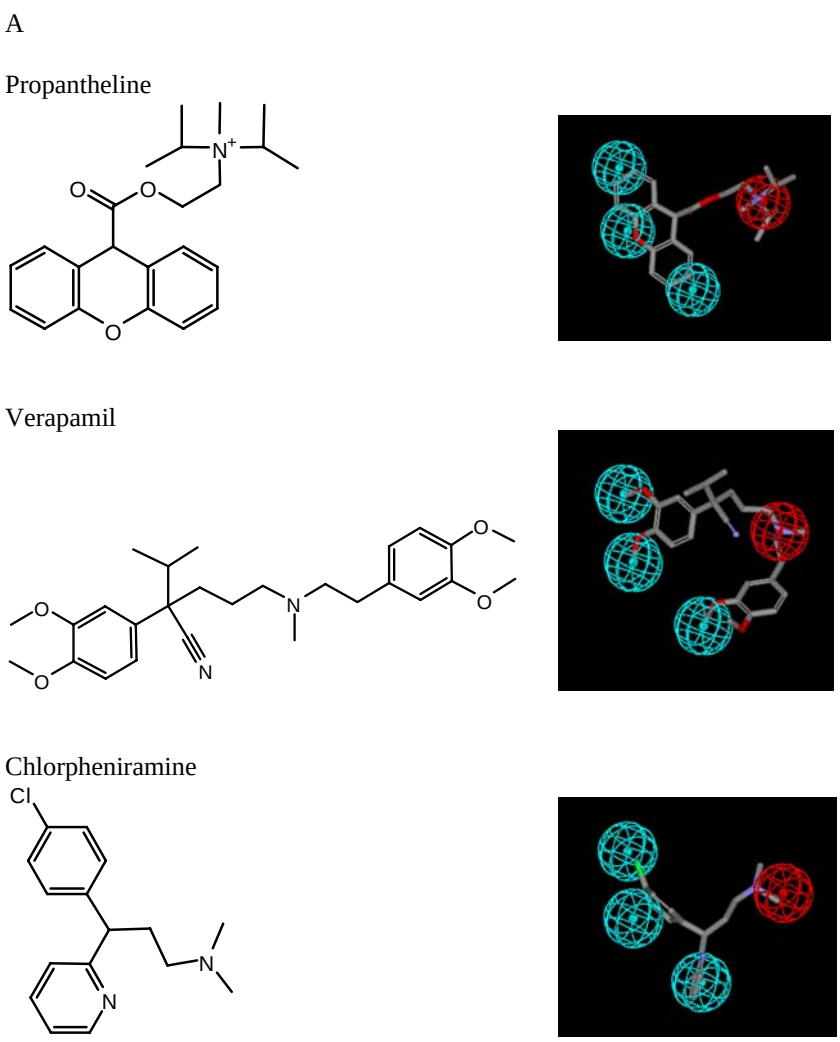

Fig. 2. HipHop pharmacophore for hOCTN2. **A** Each of the most active compounds mapped to the pharmacophore. Structures were diverse. **B** All five of the most active molecules mapped simultaneously to the pharmacophore. **C** Propantheline mapped plus the van der Waals surface to create a pharmacophore with shape restriction. Pharmacophore features represent: *cyan* hydrophobes, *red* positive ionizable which maps to the basic nitrogen.

Twelve compounds in Table II (i.e. over one third of those tested) were more potent than propantheline (percent uptake of 7.43±0.19%), which was the most potent compound from the initial screening study of 27 compounds. Twenty-seven of the 32 drugs tested (84.4%) were found to be potent inhibitors, using 40% or lower percent uptake as the criterion to denote a potent inhibitor. These results reflect the capability of the pharmacophore to predict novel and more active hOCTN2 inhibitors. It should be noted that hOCTN2-mediated translocation can be either sodium-dependent or sodium-independent (16). Experiments here employed the substrate L-carnitine, whose translocation across hOCTN2 is sodium-dependent. Hence, observations here of hOCTN2 inhibition (regardless of mechanism of inhibition) do not necessarily reflect the sodium-independent pathway, as L-carnitine is not a probe for that pathway.

An additional 21 compounds were selected for *in vitro* testing without the use of the pharmacophore (Table III). Of these compounds, only emetine (which was not in the SCUT database) mapped to the pharmacophore. Emetine inhibited OCTN2 moderately (46.9% L-carnitine uptake). Among the remaining 20 compounds which did not map to the pharmacophore, only mirtazapine was found to be potent inhibitor. These results of compounds predicted not to map to the pharmacophore further support the utility of using the OCTN2 inhibition pharmacophore for selecting compounds for testing.

Of the 53 compounds tested in Tables II and III, 33 compounds mapped to the pharmacophore, while 20 compounds did not map to the pharmacophore. Of the 33 compounds that mapped the pharmacophore, 27 inhibited hOCTN2. Of the 20 compounds that did not map to the pharmacophore, one inhibited hOCTN2. These results indicate that the pharmacophore had acceptable ability to screen for and select inhibitors over non-inhibitors.

Additionally, a pharmacophore with a van der Waals shape restriction around propantheline was also developed (Fig. 3C). The purpose of adding a shape volume was to

Diltiazem

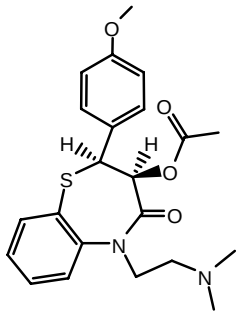

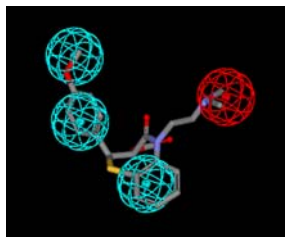

Imipramine

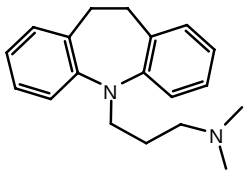

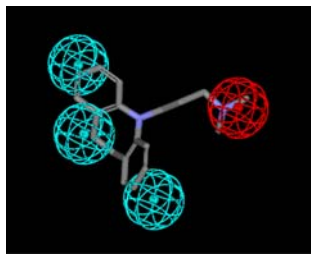

B

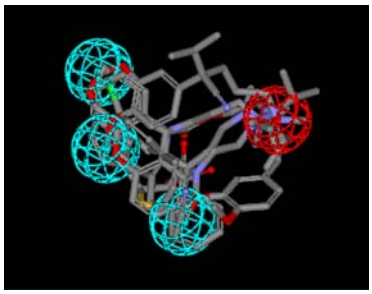

C

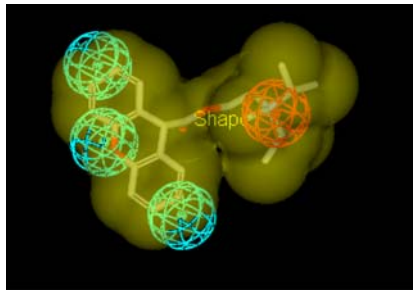

Fig. 2. (continued).

create a more restrictive features hypothesis in order to reduce the number of retrieved hits and to find molecules most similar to the shape and volume of propantheline. The pharmacophore with shape restriction identified only 49 molecules from the SCUT database (Supplemental Table III of the Electronic Supplementary Material), which were a subset of the original dataset (Supplemental Table II of the Electronic Supplementary Material). Of these 49, 17 molecules were tested *in vitro* (Supplemental Table III of the Electronic Supplementary Material), and 14 drugs (93.7%) were found to be potent inhibitors based on our selection criteria.

K_i Determination of Selected Drugs

Fourteen drugs were selected for K_i determination (Table IV). Verapamil and propantheline K_i values were measured since these compounds were the most potent from the screening studies and were used to develop the pharmacophore model. The other 12 drugs were selected since they collectively exhibited a range of percent inhibition values and FitValues. The hOCTN2 inhibition profile of vinblastine is shown in Fig. 4. The hOCTN2 pharmacophore model predicted this drug as one of the most potent inhibitors of hOCTN2. Experimentally, the K_i of vinblastine was 4.85 μM and was the most potent K_i value in this study. Vinblastine has not been previously been reported to be an OCTN2 inhibitor.

Figure 4 illustrates the Lineweaver–Burk plot of vinblastine inhibition of L-carnitine uptake. Vinblastine and L-carnitine concentrations were varied. The three lines show the linear fits to L-carnitine uptake data from experiments that employ vinblastine concentrations of 0 μM (filled circle), 50 μM (open circle) and 100 μM (filled triangle). Higher vinblastine concentration resulted in a greater slope in Fig. 4. However, the y-intercept did not change and this is consistent with a competitive inhibition model. Additionally, AIC from nonlinear regression indicated the competitive inhibition model was better fitting than the non-competitive inhibition model.

DISCUSSION

An *in silico* common features pharmacophore modeling method and an *in vitro* cell culture approach have been combined to predict the molecular requirements of hOCTN2 inhibition and identify additional drugs as novel potent

Table II. *In Vitro* Tested 32 Compounds, Selected from the 136 Compounds Retrieved by Searching the Database of 796 Compounds (656 Drugs in SCUT 2008 Database Plus Additional Drug Metabolites and Drugs of Abuse) with the HipHop Pharmacophore

Compound name	FitValue from pharmacophore	Percent L-carnitine uptake compared to control[a]
Thioridazine[b]	3.598	0.275±0.017
Vinblastine[b]	3.58	3.38±0.22
Clozapine	3.54	9.38±0.27
Amlodipine	3.527	14.4±0.5
Gefitinib	3.479	30.0±0.9 (100 μM)[a]
Trifluoperazine[b]	3.408	0.24±0.03
Dibucaine	3.404	26.3±1.3
Tamoxifen[b]	3.348	54.6±0.9 (25 μM)[a]
Amiodarone[b]	3.331	7.97±0.43 (100 μM)[a]
Atracurium	3.292	36.8±2.7
Nefazodone[b]	3.243	32.2±1.4 (50 μM)[a]
Argatroban	3.223	39.1±1.9
Pentamidine	3.083	77.2±1.9
Nelfinavir	3.005	63.7±2.0 (25 μM)[a]
Prochlorperazine[b]	3.002	0.318±0.032
Raloxifene[b]	2.954	14.4±1.3 (50 μM)[a]
Chloroquine	2.839	44.6±1.0
Metoclopramide	2.692	11.9±0.8
Desloratadine[b]	2.674	6.97±0.219
Duloxetine	2.595	15.6±0.7
Carvedilol[b]	2.593	5.64±0.34
Vancomycin	2.577	54.4±1.7
Olanzapine	2.432	32.0±0.9
Amitriptyline	2.149	22.9±0.7
Gemifloxacin	1.796	67.8±0.4
Imatinib[b]	1.759	3.98±0.22
Desipramine	1.612	32.4±0.8
Sildenafil	1.587	69.7±2.8
Quinine	1.343	14.3±0.5
Quinidine	0.955	17.2±0.6
Haloperidol	0.788	26.0±1.2
Bromocriptine[b]	0.448	34.7±1.7 (25 μM)[a]

Higher FitValues reflect greater compound fit to pharmacophore and hence predict greater hOCTN2 inhibition

[a] Extrapolated percent uptake of the compounds at 500 μM: 7.90±0.18% for gefinitib, 1.70±0.09% for amiodarone, 8.07±0.10% for nelfinavir, 2.59±0.09% for bromocriptine, 5.67±0.05% for tamoxifen, 4.53±0.14% for nefazodone, and 1.65±0.13% for raloxifene

[b] Compounds more potent than propantheline (percent uptake of 7.43±0.19%, Table I)

Table III. *In Vitro* Tested Additional 21 Compounds, Including Carnitine Mimics, Literature Reported OCTN2 Inhibitors and Drugs Causing Rhabdomyolysis

Compound name	FitValue from pharmacophore	Percent L-carnitine uptake compared to control
Emetine	3.857	46.9±2.8
Mirtazapine	No map	27.8±2.3
Betaine	No map	40.5±0.2
Cerivastatin[a]	No map	43.4±2.1
Pyrilamine	No map	51.7±1.6
Citalopram	No map	52.6±2.0
Cephaloridine	No map	53.2±0.8
Cimetidine	No map	54.1±2.6
Atorvastatin[a]	No map	57.2±2.0
Edrophonium	No map	60.1±1.0
Venlafaxine	No map	69.9±3.1
Bethanechol	No map	74.1±1.6
Choline	No map	76.0±2.2
Cyclopentolate	No map	76.9±2.2
Ketorolac	No map	82.1±0.4
Gabapentin	No map	83.6±3.5
Levofloxacin[a]	No map	85.0±0.3
Succinylcholine[a]	No map	89.0±2.1
Lomefloxacin	No map	92.3±5.2
Procarbazine	No map	88.3±2.8
Lisinopril	No map	114±3

These compounds were not retrieved by pharmacophore searching of the database of 796 compounds (656 drugs in SCUT 2008 database plus additional drug metabolites and drugs of abuse). Except for emetine, which was not in SCUT 2008 database, none of the compounds mapped to the pharmacophore

[a] Compounds that have been previously shown to cause rhabdomyolysis

inhibitors of hOCTN2. Some of the most potent hOCTN2 inhibitors reflect diverse classes of molecules, both structurally and therapeutically, such as phenothiazine antipsychotics, atypical antipsychotics, selective estrogen receptor modulators, calcium channel blockers, anti-cancer compounds, and tricyclic antidepressants.

Pharmacological Implications of hOCTN2 Inhibition

Considering the physiologically important role of hOCTN2 in carnitine transport as well as the widespread expression of hOCTN2 in human tissues (1), the high affinity inhibition of hOCTN2 of these therapeutic agents may have pharmacological implications. Secondary carnitine deficiency is known to be induced by long-term treatment of various drugs such as emetine (17) and cephaloridine (11). One suggested mechanism is the inhibition of hOCTN2-mediated L-carnitine uptake into various tissues, especially kidney, heart, and skeletal muscle, where hOCTN2 is highly expressed. Studies have shown that cephaloridine enhances renal excretion of carnitine, consistent with the inhibition of carnitine renal re-absorption by cephaloridine (18,19). *In*

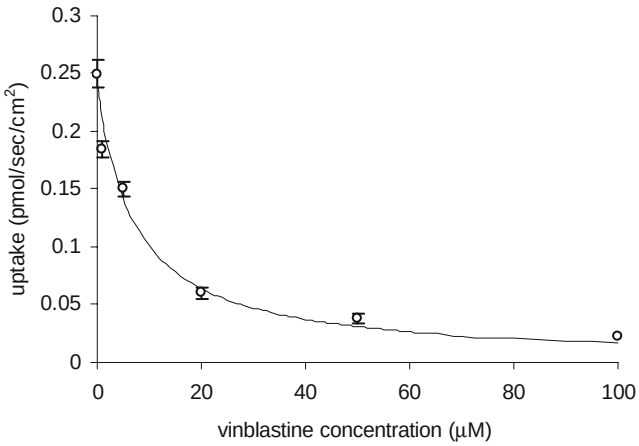

Fig. 3. Inhibition of hOCTN2 by vinblastine. L-carnitine uptake was reduced in the presence of vinblastine. SCUT database screening of the pharmacophore predicted vinblastine to inhibit hOCTN2. Vinblastine inhibited hOCTN2 with K_i=4.85±0.71 μM.

Table IV. Competitive Inhibitory K_i Values

Compound name	FitValue from pharmacophore	Competitive inhibitory K_i value (μM)
Vinblastine	3.580	4.85±0.71
Carvedilol	2.593	10.7±1.6
Raloxifene	2.954	13.8±2.4
Bromocriptine	0.448	16.6±2.0
Verapamil	3.714	17.6±3.1
Propantheline	1.4	20.4±4.1
Thioridazine	3.598	23.0±4.1
Clozapine	3.540	47.3±8.6
Prochlorperazine	3.002	51.3±10.5
Desloratadine	2.674	53.3±6.7
Trifluoperazine	3.408	67.3±10.1
Amlodipine	3.527	96.0±15.2
Duloxetine	2.595	118±13
Cerivastatin	No map	425±12

vitro Hela cell line studies have demonstrated that cephaloridine is a potent hOCTN2 inhibitor ($IC_{50} = 0.79 \pm 0.10\ mM$), as well as a substrate (11).

Since carnitine deficiency is linked with rhabdomyolysis (20,21), hOCTN2 inhibition might also be a possible contributor to drug-induced rhabdomyolysis since hOCTN2 inhibition might limit L-carnitine uptake. We have considered the possible association between clinical rhabdomyolysis and hOCTN2 inhibition by compiling a list of those compounds that were found to be the most potent inhibitors and least potent inhibitors *in vitro*, as well as compounds whose K_i values were determined (Table V). The C_{max}/K_i ratio was also computed as a potential predictor for clinical rhabdomyolysis. Among the 12 compounds that were associated with rhabdomyolysis, ten (83.3%) have a C_{max}/K_i ratio higher than 0.0025. This ratio of 0.0025 separates the top half of C_{max}/K_i values from the bottom half of C_{max}/K_i values. In contrast, among 21 compounds that were not associated with rhabdomyolysis, only six (28.6%) have a C_{max}/K_i ratio higher than 0.0025. Clinical rhabdomyolysis was associated with a C_{max}/K_i value above 0.0025 (Pearson's chi-square test $p=0.00247$).

HMG-CoA reductase inhibitors are well known to cause rhabdomyolysis. Cerivastatin was removed from the market due to this side effect. FDA recently issued an alert for the risk of rhabdomyolysis when simvastatin is administered with amiodarone. In the present study, both cerivastatin and atorvastatin were found to be inhibitors of hOCTN2. The K_i of cerivastatin was 425±12 μM. Amiodarone inhibited hOCTN2 at a low micromolar concentration.

While clinical rhabdomyolysis was associated with a C_{max}/K_i value above 0.0025, it should be emphasized that the use of C_{max}/K_i as a predictor would result in false positives (e.g. rifampin) and false negatives (e.g. selegiline). If one were to extrapolate pharmacophore performance to rhabdomyolysis, the pharmacophore would exhibit false positives and false negatives. For example, succinylcholine, cerivastatin, levofloxacin, and selegiline did not map the pharmacophore, although are associated with rhabdomyolysis. However, the pharmacophore did successfully retrieve amiodarone, nelfinavir, thioridazine, nefazodone, and clozapine for *in vitro* testing, all of which yielded C_{max}/K_i values above 0.0025 and are associated with rhabdomyolysis.

This observed association between rhabdomyolysis and C_{max}/K_i is preliminary and perhaps should only be interpreted as an ongoing effort to leverage cell culture methods to screen for transporter-mediated drug side effects. While laboratory methods have been improved to anticipate metabolism-based drug–drug interactions (22), predictability for drug side effects and drug–drug interactions from transporter assays is not well developed. Further evidence is needed to better assess an association between rhabdomyolysis and C_{max}/K_i. For example, direct association between drug plasma level and reduced tissue L-carnitine level may merit subsequent study. A rationale for a specific C_{max}/K_i value that considers drug pharmacokinetics (e.g. tissue distribution, plasma protein binding) would also be advantageous, as a C_{max}/K_i value

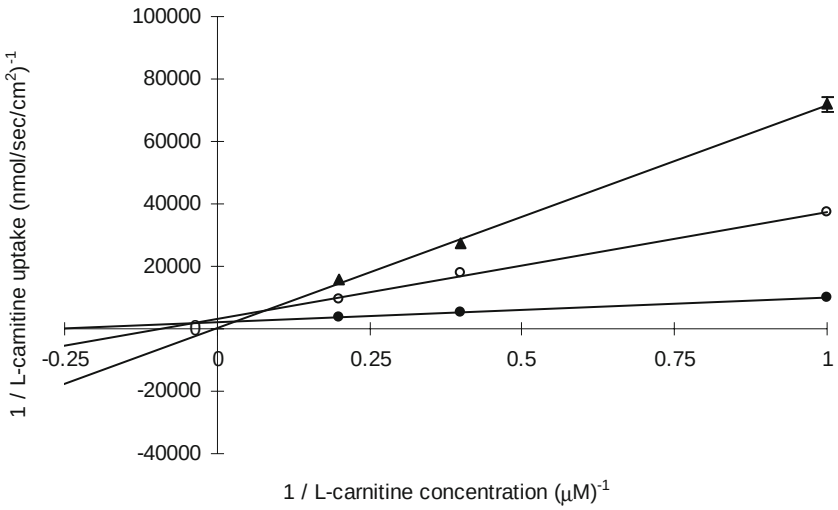

Fig. 4. Lineweaver–Burk plot of vinblastine inhibition of L-carnitine uptake. Vinblastine (0, 50, and 100 μM) and L-carnitine (1, 2.5, and 5 μM) concentrations were varied. The three *lines* show the linear fits to L-carnitine uptake data from experiments that employed vinblastine concentrations of 0 μM (*filled circle*), 50 μM (*open circle*), and 100 μM (*filled triangle*).

Table V. Possible Association between Clinical Rhabdomyolysis and hOCTN2 Inhibition

Compound name	Percent of uptake at 500 μM inhibitor	K_i or estimated K_i (μM)[a]	Documented to cause rhabdomyolysis in the literature	C_{max} (μM)[b]	C_{max}/K_i
Amiodarone	1.70±0.09	5.72	Yes with simvastatin (1)	3.43	0.600
Nelfinavir	8.07±0.10	29.2	Yes with simvastatin (2)	10.2	0.349
Thioridazine	0.275±0.017	23.0±4.1	Yes (3)	6.75	0.293
Nefazodone	4.53±0.14	15.7	Yes with simvastatin (4)	2.62	0.167
Rifampin	77.6±4.3	1,150	No	8.82	0.0767
Succinylcholine	89.0±2.1	2,700	Yes (5)	180	0.0667
Propantheline	7.43±0.19	20.4±4.1	No	1.06	0.0519
Cerivastatin	43.4±2.1	425±12	Yes (6)	19.6	0.0461
Clozapine	9.38±0.27	47.3±8.6	Yes (7)	1.72	0.0364
Verapamil	9.49±0.18	17.6±3.1	Yes with trandolapril (8)	0.306	0.0174
Gefinitib	7.90±0.18	29	No	0.474	0.0164
Carvedilol	5.64±0.34	10.7±1.6	No	0.131	0.0123
Tamoxifen	5.67±0.05	20	No	0.171	0.00854
Levofloxacin	85.0±0.3	1,900	Yes (9)	14.4	0.00756
Lomefloxacin	92.3±5.2	4,000	No	10.5	0.00263
Lamivudine	88.6±3.9	2,590	Yes (10)	6.67	0.00258
Ketorolac	82.1±0.4	1,530	No	3.36	0.00220
Acyclovir	93.9±2.7	5,130	No	7.16	0.00140
Vinblastine	3.38±0.22	4.85±0.71	No	0.00604	0.00125
Procarbazine	88.3±2.8	2,520	No	3.13	0.00124
Duloxetine	15.6±0.7	118±13	No	0.122	0.00103
Erythromycin	89.6±2.4	2,870	Yes with simvastatin (11)	2.23	7.77×10^{-4}
Desloratadine	6.97±0.219	53.3±6.7	No	0.0335	6.28×10^{-4}
Hydrochlorothiazide	92.5±0.6	4,110	No	1.65	4.01×10^{-4}
Prochlorperazine	0.318±0.032	51.3±10.5	No	0.0168	3.27×10^{-4}
Atenolol	96.0±5.5	8,000	No	1.13	1.41×10^{-4}
Raloxifene	1.65±0.13	13.8±2.4	No	0.00148	1.07×10^{-4}
Amlodipine	14.4±0.5	96.0±15.2	No	0.0000810	8.43×10^{-5}
Trifluoperazine	0.24±0.03	67.3±10.1	No	0.00528	7.85×10^{-5}
Bromocriptine	2.59±0.09	16.6±2.0	No	0.000959	5.78×10^{-5}
Selegiline	78.7±2.2	1,230	Yes (12)	0.0244	1.98×10^{-5}
Atropine	92.3±3.5	4,000	No	0.0332	8.30×10^{-6}
Zidovudine	86.5±1.8	2,140	No	0.0124	5.79×10^{-6}

C_{max}/K_i was computed for some most potent inhibitors and least potent inhibitors, as well as all the remaining compounds that have the K_i determined. See Supplemental Table IV of the Electronic Supplementary Material for references 1–45

[a] For the compounds whose K_i were not determined experimentally, estimated K_i was computed using screening data and Eq. 3 in the "MATERIALS AND METHODS" section

[b] Values for C_{max} in units of micromolar were computed using compound molecular weight and C_{max} from the literature. References 13–45 provide literature C_{max} values for listed compounds, respectively

of 0.0025 is applied here since this value separated the top half drugs from bottom half drugs in Table V.

Pharmacophore Testing

A common features pharmacophore was developed and consisted of three hydrophobic features and a positive ionizable feature (Fig. 2). These features are thus expected to be important for molecular interactions with hOCTN2. Of course, it is possible that in the resultant pharmacophore, not all of the pharmacophore features are important as they are just "common features" in the actives.

The pharmacophore models with and without shape restriction performed similarly and had very few false positives. However, the predictive power of the two pharmacophore models differed in terms of retrieving the five active drugs in the training set. While the pharmacophore without shape restriction retrieved four of the five drugs (it is uncertain why it failed with propantheline), the pharmacophore with the van der Waals shape restriction only retrieved imipramine. Moreover, the latter pharmacophore with shape restriction missed identifying several compounds that were subsequently found to be potent novel inhibitors, such as vinblastine and amlodipine, which were found with the pharmacophore without shape restriction. These results indicate pharmacophore with shape restriction is too restrictive in terms of shape, reliant on propantheline. Therefore, the pharmacophore without shape restriction was used to obtain FitValues for all database compounds, and is viewed here as the preferred pharmacophore to date for screening. However, the shape restricted pharmacophore still demonstrated a much higher percent active rate than the pharmacophore alone. This shape restricted pharmacophore approach might be useful if much larger databases were to be screened as this latter pharmacophore has the potential to retrieve hit lists approximately one third the size of the other pharmacophore with a higher level of true positives.

One report investigated the structural requirements of hOCTN2 inhibition using L-carnitine and cephaloridine as training compounds to derive a pharmacophore that was used

to search the Merck Index (23). The pharmacophore included a constantly positively charged nitrogen atom and a carboxyl, nitrile or ester group connected by a two- to four-atom linker. The majority of the compounds retrieved were carnitine mimics. The pharmacophore search appeared to yield fewer, less chemically diverse, less potent, and much less drug-like compounds than reported here in the present study. Additionally, since hOCTN2-mediated carnitine uptake is sodium-dependent while hOCTN2-mediated cation uptake is sodium-independent, the recognition site of cations and carnitine may not significantly overlap.

Two missense mutations of OCTN2 (i.e. L352R, P478L) causing primary carnitine deficiency have been tested *in vitro* and result in complete loss of carnitine transport function. However, only the L352R mutant was associated with loss of organic cation transport function, whereas the P478L mutant had higher organic cation transport activity than the wild type OCTN2 (24). Hence, the superposition of L-carnitine with cephaloridine to derive the previously reported pharmacophore may be less applicable to drugs, since the pharmacophore for carnitine mimics and diverse cation/zwitterion drugs might be different overall. For example, verapamil was discussed in the report as a molecule that does not follow their pharmacophore since verapamil lacks a permanent positive charge but behaves as a potent inhibitor (23). Meanwhile, verapamil was used to derive our pharmacophore. It would therefore indicate that we are potentially modeling a unique, or a partially overlapping site in this study, compared to the previous published pharmacophore. The retrieval of diverse and potent inhibitors by our model also indicates it is well validated, in contrast to the previous model.

In summary, hOCTN2 inhibition molecular requirements were elucidated by the integration of computational modeling and *in vitro* testing. Twenty-seven drugs were screened initially for their potential to inhibit uptake of L-carnitine. A common features pharmacophore was also used to search a database of compounds. Fifty-three drugs, including some predicted not to be inhibitors, were subsequently selected and screened *in vitro* to test the pharmacophore. The pharmacophore performed exceptionally well predicting 27 out of 33 drugs as hOCTN2 inhibitors *in vitro*. Diverse therapeutic classes of drugs were also found to be low micromolar inhibitors, including many drugs not previously known to inhibit hOCTN2. This validation suggests that the pharmacophore consisting of three hydrophobic features ~7 to 9.4 Å from a positive ionizable feature captures important interactions between OCTN2 inhibitors and the transporter. The findings in this study may also have clinical implications for drug interactions mediated by compounds inhibiting hOCTN2.

ACKNOWLEDGMENTS

This work was supported in part by National Institutes of Health grant DK67530. The authors kindly acknowledge Dr. Xin Ming and Dr. Dhiren R. Thakker (University of North Carolina-Chapel Hill) for providing the hOCTN2-MDCK cell line used in this study. The authors gratefully acknowledge Dr. Matthew D. Krasowski for his assistance in creating the SCUT 2008 database supplemented with metabolites and drugs of abuse. The authors also thank Accelrys, San Diego, CA for making Discovery Studio Catalyst available.

REFERENCES

1. Dresser MJ, Leabman MK, Giacomini KM. Transporters involved in the elimination of drugs in the kidney: organic anion transporters and organic cation transporters. J Pharm Sci. 2001;90(4):397–421. doi:10.1002/1520-6017(200104)90:4<397::AID-JPS1000>3.0.CO;2-D
2. Rebouche CJ, Paulson DJ. Carnitine metabolism and function in humans. Annu Rev Nutr. 1986;6:41–66. doi:10.1146/annurev.nu.06.070186.000353.
3. Matsuishi T, Yoshino M, Kato H, Ohura T, Tsujimoto G, Hayakawa J, *et al.* Primary systemic carnitine deficiency is caused by mutations in a gene encoding sodium ion-dependent carnitine transporter. Nat Genet. 1999;21(1):91–4. doi:10.1038/5030.
4. Wang Y, Ye J, Ganapathy V, Longo N. Mutations in the organic cation/carnitine transporter OCTN2 in primary carnitine deficiency. Proc Natl Acad Sci U S A. 1999;96(5):2356–60. doi:10.1073/pnas.96.5.2356.
5. Christopher-Stine L. Statin myopathy: an update. Curr Opin Rheumatol. 2006;18(6):647–53.
6. Ohashi R, Tamai I, Yabuuchi H, Nezu JI, Oku A, Sai Y, *et al.* Na(+)-dependent carnitine transport by organic cation transporter (OCTN2): its pharmacological and toxicological relevance. J Pharmacol Exp Ther. 1999;291:778–84.
7. Grube M, Meyer zu Schwabedissen HE, Präger D, Haney J, Möritz KU, Meissner K, *et al.* Uptake of cardiovascular drugs into the human heart: expression, regulation, and function of the carnitine transporter OCTN2 (SLC22A5). Circulation 2006;113(8):1114–22.
8. Wagner CA, Lukewille U, Kaltenbach S, Moschen I, Broer A, Risler T, *et al.* Functional and pharmacological characterization of human Na(+)-carnitine cotransporter hOCTN2. Am J Physiol Renal Physiol. 2000;279:F584–591.
9. Clement OO, Mehl AT. HipHop: pharmacophore based on multiple common-feature alignments. In: Guner OF, editor. Pharmacophore perception, development, and use in drug design. San Diego: IUL; 2000. p. 69–84.
10. Ekins S, Chang C, Mani S, Krasowski MD, Reschly EJ, Iyer M, *et al.* Human pregnane X receptor antagonists and agonists define molecular requirements for different binding sites. Mol Pharmacol. 2007;72:592–603. doi:10.1124/mol.107.038398.
11. Ganapathy ME, Huang W, Rajan DP, Carter AL, Sugawara M, Iseki K, *et al.* Beta-lactam antibiotics as substrates for OCTN2, an organic cation/carnitine transporter. J Biol Chem. 2000;275:1699–707.
12. Chang C, Ekins S, Bahadduri P, Swaan PW. Pharmacophore-based discovery of ligands for drug transporters. Adv Drug Deliv Rev. 2006a;58:1431–50.
13. Chang C, Bahadduri PM, Polli JE, Swaan PW, Ekins S. Rapid identification of P-glycoprotein substrates and inhibitors. Drug Metab Dispos. 2006b;34(12):1976–84.
14. Ekins S, Johnston JS, Bahadduri P, D'Souzza VM, Ray A, Chang C, Swaan PW. *In vitro* and pharmacophore based discovery of novel hPEPT1 inhibitors. Pharm Res. 2005;22:512–7.
15. Akarawut W, Lin CJ, Smith DE. Noncompetitive inhibition of glycylsarcosine transport by quinapril in rabbit renal brush border membrane vesicles: effect on high-affinity peptide transporter. J Pharmacol Exp Ther. 1998;287(2):684–90.
16. Koepsell H, Lips K, Volk C. Polyspecific organic cation transporters: structure, function, physiological roles, and biopharmaceutical implications. Pharm Res. 2007;24(7):1227–51.
17. Kuntzer T, Reichmann H, Bogousslavsky J, Regli F. Emetine-induced myopathy and carnitine deficiency. J Neurol. 1990;237:495–6.
18. Tune BM. Effects of L-carnitine on the renal tubular transport of cephaloridine. Biochem Pharmacol. 1995;50(4):562–4.
19. Tune BM, Hsu CY. Toxicity of cephaloridine to carnitine transport and fatty acid metabolism in rabbit renal cortical mitochondria: structure-activity relationships. J Pharmacol Exp Ther. 1994;270(3):873–80.

20. Luck RP, Verbin S. Rhabdomyolysis: a review of clinical presentation, etiology, diagnosis, and management. Pediatr Emerg Care 2008;24(4):262–8.
21. Morris AA, Turnbull DM. Fatty acid oxidation defects in muscle. Curr Opin Neurol. 1998;11(5):485–90.
22. Fowler S, Zhang H. *In vitro* evaluation of reversible and irreversible cytochrome P450 inhibition: current status on methodologies and their utility for predicting drug–drug interactions. AAPS J. 2008;10(2):410–24.
23. Todesco L, Bur D, Brooks H, Török M, Landmann L, Stieger B, *et al.* Pharmacological manipulation of L-carnitine transport into L6 cells with stable overexpression of human OCTN2. Cell Mol Life Sci. 2008;65(10):1596–608.
24. Seth P, Wu X, Huang W, Leibach FH, Ganapathy V. Mutations in novel organic cation transporter (OCTN2), an organic cation/carnitine transporter, with differential effects on the organic cation transport function and the carnitine transport function. J Biol Chem. 1999;274(47):33388–92.